Supplemental Information for:

Trailing the heat: Eurasian Teal (*Anas crecca*) schedule their spring migration basing on the increase in soil temperatures along the route

Table of Contents:

Tracking data

The tracking data was filtered using the Hybrid Douglas Filter available in Movebank (Douglas et al. 2012). We identified the individual wintering area as the site where the teal was captured and where its movements between successive locations were < 24 km. Migration was considered started when the individual made a movement of > 24 km, directed towards the breeding grounds without any return to the initial area (for a detailed explanation of this criterion, see Cerritelli et al. 2020). This approach was necessary for two reasons: i) some teal flew more than 24 km from the first residency area identified but then returned to stay for a long time in a site close to the first one (distance between areas: median = 35.4 km; IQR = 8 – 53.2 km); ii) some individuals were not oriented towards the breeding grounds (heading South or West) during their first movement. Stopover areas were identified as sites where birds remained > 48 h and moved < 24 km between successive locations. Breeding sites were identified as areas where teal showed restricted movements (< 4 km) and remained for more than 1 month.

Selection of pressure level for the wind components

To select the appropriate pressure level of the wind components, we performed a preliminary analysis. As flight altitude measurements for free-ranging teal were not available, we compared models that included wind components at the three lowest altitude levels (1000, 975 and 950 mPa), among the pressure levels available in the dataset used. We made this choice based on the only available flight altitude information for ducks obtained through radar tracking (Guillemain and Elmberg 2014) and on previous works on birds of similar body mass and flight as teal, which investigated the effect of winds during migration (Gill et al. 2014). Nevertheless, we did not detect any difference among the three models and thus opted to include the 1000mPa level of wind components in all subsequent analyses.

Statistical analysis

Departure from wintering sites

We first checked for correlation between variables using Spearman correlation, ensuring that we did not include variables that were highly correlated (more than 0.50) in the same model. To assess the possible effects of environmental cues on departure probability we used a Cox-proportional hazard model (Cox 1972). This non-parametric model estimates the probability, per unit of time, of an event (in this case, "departure") occurring as a function of the baseline hazard, which can be modified by a set of fixed or time-dependent explanatory variables, such as environmental conditions experienced by birds in their wintering site. The analysis included all tracked teal (n = 30), including those that did not complete migration. For the two individuals tracked over three successive years, we only included data from one year, which was randomly sampled (year 2016 for TUS04 and year 2014 for VEN05).

We constructed a base model with the environmental variables that should affect the departure decision, based on literature. Since photoperiod plays a crucial role in bird migration (Berthold 1996) we included in this model the hours of light per day (day length), estimated using R package "geosphere" ver. 1.5-14 (Hijmans 2021). Temperature may also play a crucial role in departure from wintering site, as it may indicate the advancement of the spring season (e.g., Bauer et al. 2008; Weller et al. 2022). Because the mean soil temperature was correlated with daylength ($r_s = 0.61$), we considered the effect of temperature as the residuals of a linear regression between daily soil temperature and day of the year (residual soil temperature, RSoilTemp). We performed the linear regression for each wintering area (Friuli, Veneto, Tuscany, Lombardy and Puglia), including data from all years of tracking (2014 - 2018) only for the period that included the last wintering phase and the departures of all animals (1 January to 31 March). By doing this, we tested the effect of relatively anomalous temperature (temperatures above the average of the period, in particular) experienced by the animals during the last part of the wintering period, rather than the effect of temperature per se (Linek et al. 2021). Finally, we included the wind v-component (North-South component of the wind vector) in the base model, because many bird species prefer to start migratory flights with favourable wind conditions (e.g., Liechti et al. 2006; Gill et al. 2014). Positive values of the wind v-component (winds with a South-North direction) should represent favourable winds. We expected that the wind u-component (West-East component of the wind vector) would be less important than the v-component, given the main northward component of migratory tracks of tagged teal, and thus did not include it in the base model. The individuals were included in the model as clusters.

Given the available sample of individuals and the correlation among several of meteorological variables (Fig. S3), we added one of the remaining meteorological variables (wind u-component, cloud cover, precipitation, atmospheric pressure and relative humidity) at a time to the base model (i.e., the model including photoperiod, RSoilTemp and wind v-components) to avoid overparametrization (Anderson and Burnham 2002). Model selection was performed using the Akaike Information Criterion corrected for small sample size (AICc, Anderson and Burnham 2002). We considered models within two AICc units from the best models to be equivalent (Anderson and Burnham 2002) unless they differed only for one additional parameter which was considered uninformative (Arnold 2010). All variables were centered before the analysis (Schielzeth 2010). Model significance was tested by means of the Wald test. Collinearity and other model assumptions were checked according to Therneau and Grambsch (2000) using package "survminer" ver. 0.4.9 (Kassambara et al. 2021) and "rms" ver. 6.3-0 (Harrell 2022).

Analysing departure from stopover

The variables considered in this analysis included Defrost Degree Day (DDD), total precipitation, atmospheric pressure, cloud cover and wind components. DDD is a modification of Growing Degree Days (GDD) that was previously used in studies investigating the possible effect of vegetation growth on the departure decision of migratory geese (e.g., van Wijk et al. 2012; Lameris et al. 2017). DDD was used as a proxy for food availability, as teal feed on both seeds and invertebrates during spring migration (Guillemain and Elmberg 2014). To calculate the yearly Defrost Degree Day (DDD) for each stopover site, we followed the method described by van Wijk et al. (2012). Specifically, we used the daily temperatures of the first soil level (0 - 7 cm) and identified the soil temperature of the day when ground thawing started in the area as the threshold temperature (TBASE). This was determined as the first day that thaw ground was recorded in the satellite data followed by at least 10 days of absence of freeze. Given the large range of latitudes involved, we used a different TBASE for each stopover. Finally, we extracted the DDD values for the days when the teal were residing in the stopover.

We did not include photoperiod in our analysis due to the variability in day length during migration caused by both seasonal progression and changes in bird latitude, resulting in significant heterogeneity among different stopovers. Nonetheless, we did not anticipate photoperiod to be a significant cue for the birds' departure decisions from stopover sites. Photoperiod serves as a proxy for time of year, indicating the time frame during which birds can prepare for and initiate migration (Berthold 1996; Akesson et al. 2017; Akesson and Helm 2020). As observed in Pink-footed geese (Bauer et al. 2008), once migration started birds do not use photoperiod to regulate their migration speed.

Some meteorological variables showed high degrees of correlation (Fig. S4), like cloud cover with precipitation ($r_s = 0.53$) and relative humidity ($r_s = 0.51$), and precipitation with relative humidity ($r_s = 0.72$). This high level of correlation was considered when constructing the model (see below). All variables were centered before the analysis (Schielzeth 2010). The analysis was done using Generalized Estimating Equations (GEE; Hardin & Hilbe 2002) with a binomial error distribution and an AR1 correlation structure to take into account the temporal autocorrelation of the data. The model was fitted using package “wgeesel” ver. 1.5 (Xu et al. 2018) and individuals were included in the model as clusters. The analysis was carried out on the 21 that completed migration, and when the same individual was tracked for multiple years, we included data from only one year randomly sampled (year 2016 for TUS04 and year 2014 for VEN05). To avoid model overparametrization and given the high level of correlation between some meteorological variables, we performed model selection using the same approach used in the previous analysis. We started with a base model including DDD and wind v-component, which we hypothesized would have the most significant effect on teal decision to continue migration. Then we added one of the remaining meteorological variables at time. The best model was selected according to the Quasi-likelihood under the independence model Information Criterion (QIC, Hardin & Hilbe 2002). Model assumptions were checked using “DHARMa” ver. 0.4.5 (Hartig 2022), and marginal R^2 (Zheng 2000) was estimated using package “wgeesel” ver. 1.5 (Xu et al. 2018).

References

Åkesson S, Helm B, 2020. Endogenous programs and flexibility in bird migration. *Frontiers in Ecology and Evolution*, 8:78. https://doi.org/10.3389/fevo.2020.00078

Åkesson S, Ilieva M, Karagicheva J, Rakhimberdiev E, Tomotani B, Helm B, 2017. Timing avian long-distance migration: from internal clock mechanisms to global flights. *Philosophical*

Transactions of the Royal Society B: Biological Sciences, 372:20160252. https://doi.org/10.1098/rstb.2016.0252

Anderson DR, Burnham KP, 2002. Avoiding Pitfalls When Using Information-Theoretic Methods. *The Journal of Wildlife Management*, 66:912–918. https://doi.org/10.2307/3803155

Arnold TW, 2010. Uninformative parameters and model selection using Akaike' s information criterion. *Journal of Wildlife Management*, 74:1175-1178. https ://doi.org/10.2193/2009-367

Bauer S, Gienapp P, Madsen J, 2008. The relevance of environmental conditions for departure decision changes en route in migrating geese. *Ecology*, 89:1953-1960. https://doi.org/10.1890/07-1101.1

Berthold P, 1996. Control of bird migration. Springer Science & Business Media.

Cerritelli G, Vanni L, Baldaccini NE, Lenzoni A, Sorrenti, M., et al., (2020). Simpler methods can outperform more sophisticated ones when assessing bird migration starting date. *Journal of Ornithology*, 161:901-907.

Cox DR, 1972. Regression Models and Life-Tables. *Journal of the Royal Statistical Society*. *Series B (Methodological)*, 34:187-220 http://www.jstor.org/stable/2985181. Accessed 21 Nov. 2022.

Douglas DC, Weinzierl RC, Davidson S, Kays R. Wikelski M, Bohrer G, 2012. Moderating Argos location errors in animal tracking data. *Methods in Ecology and Evolution,* 3:999-1007. https://doi.org/10.1111/j.2041-210X.2012.00245.x

Gill Jr RE, Douglas DC, Handel CM, Tibbitts TL, Hufford G et al., 2014. Hemispheric-scale wind selection facilitates bar-tailed godwit circum-migration of the Pacific. *Animal Behaviour*, 90:117-130. 10.1016/j.anbehav.2014.01.020

Giunchi D, Baldaccini NE, Lenzoni A, Luschi P, Sorrenti M et al., 2019. Spring migratory routes and stopover duration of satellite-tracked Eurasian Teals *Anas crecca* wintering in Italy. *Ibis*, 161:117-130. https://doi.org/10.1111/ibi.12602

Guillemain M, Elmberg J, 2014. *The teal*. Bloomsbury Publishing. London

Harrell Jr FE, 2022. rms: Regression Modeling Strategies. R package version 6.3-0, <https://CRAN.R-project.org/package=rms>.

Hardin JW, Hilbe JM, 2002. *Generalized estimating equations*. Chapman and Hall/CRC

Hartig F, 2022. DHARMa: Residual Diagnostics for Hierarchical (Multi-Level /Mixed) Regression Models. R package version 0.4.5, <https://CRAN.R-project.org/package=DHARMa>

Hijmans R, 2021. geosphere: Spherical Trigonometry. R package version 1.5-14, <https://CRAN.R-project.org/package=geosphere>.

Kassambara A, Kosinski M, Biecek P, 2021. survminer: Drawing Survival Curves using 'ggplot2'. R package version 0.4.9, <https://CRAN.R-project.org/package=survminer>.

Liechti F, 2006. Birds: blowin’ by the wind? Journal of Ornithology, 147:202-211. https://doi.org/10.1007/s10336-006-0061-9

Linek N, Brzęk P, Gienapp P, O’Mara MT, Pokrovsky I, Schmidt A, Shipley JR, et al, 2021. A Partial Migrant Relies upon a Range-Wide Cue Set but Uses Population-Specific Weighting for Migratory Timing. Movement Ecology 9: 63. https://doi.org/10.1186/s40462-021-00298-y.

Lameris TK, Jochems F, van der Graaf AJ, Andersson M, Limpens J et al., 2017. Forage plants of an Arctic-nesting herbivore show larger warming response in breeding than wintering grounds, potentially disrupting migration phenology. Ecology and Evolution, 7:2652-2660. https://doi.org/10.1002/ece3.2859

Schielzeth H, 2010. Simple means to improve the interpretability of regression coefficients. Methods in Ecology and Evolution 1:103-113. https://doi.org/10.1111/j.2041-210X.2010.00012.x

Therneau TM, Grambsch PM, 2000. *Modeling survival data: extending the Cox model.* Springer, New York.

Van Wijk RE, Kölzsch A, Kruckenberg H, Ebbinge BS, Müskens GJDM, et al., 2012. Individually tracked geese follow peaks of temperature acceleration during spring migration. *Oikos*, 121: 655-664. https://doi.org/10.1111/j.1600-0706.2011.20083.x

Weller FG, Beatty WS, Webb EB, Kesler DC, Krementz DG, Asante K, Naylor LW, 2022. Environmental drivers of autumn migration departure decisions in midcontinental mallards. Movement Ecology 10: 1. https://doi.org/10.1186/s40462-021-00299-x

Xu C, Li Z, Wang M, 2018. wgeesel: Weighted Generalized Estimating Equations and Model Selection. R package version 1.5, <https://CRAN.R-project.org/package=wgeesel>.

Zheng B, 2000. Summarizing the goodness of fit on generalized linear models for longitudinal data. *Statistics in Medicine*, 19:1265-1275. https://doi.org/10.1002/(SICI)1097-0258(20000530)19:10<1265::AID-SIM486>3.0.CO;2-U

Table S1. Summary information for tracked teals. IDs marked with an asterisk refer to individuals tracked for successive years. In these cases, we included in the models the data for just one year randomly sampled: year 2016 for TUS4 and year 2014 for VEN 05. Three different duty cycles of Argos satellite transmitters (PTT) were used: 6/16 = 6 hours on/16 hours off, 10/48 = 10 hours on/48 hours off, 10/48 on-off = 10 hours on/48 hours off, but the PTT was activated whenever it reached a sufficient charging level, even before the end of the 48 hour "off" period. For the attachment procedures please refer to Giunchi et al. (2019).

ID	Sex	Weight (g)	Date of capture	Capture site	PTT duty cycle	Tracking duration (days)
FRI02	F	326	22/01/2018	Valle Pantani (UD)	10/48 on-off	334
LOM02	F	260	06/01/2014	Quinzano d'Oglio (BS)	10/48	342
LOM03	F	250	13/01/2015	Quinzano d'Oglio (BS)	6/16	147
LOM04[†]	F	285	25/01/2015	Quinzano d'Oglio (BS)	6/16	86
LOM05	F	235	16/01/2016	Gambara (BS)	10/48 on-off	272
LOM07	F	336	03/01/2017	Clusane (BS)	10/48 on-off	294
PUG01[†]	M	290	23/01/2016	S. Giovanni Rotondo (FG)	10/48 on-off	40
TUS01[†]	F	290	28/12/2013	San Rossore (PI)	10/48	153
TUS04*	F	299	07/01/2014	San Rossore (PI)	10/48	817
TUS06[†]	F	269	31/12/2014	San Rossore (PI)	6/16	137
TUS09	F	342	08/01/2015	San Rossore (PI)	6/16	248
TUS10[†]	F	298	12/01/2015	San Rossore (PI)	6/16	105
TUS14	F	306	06/02/2018	San Rossore (PI)	10/48 on-off	205
VEN01	F	314	13/01/2014	Valle Morosina (PD)	10/48	352
VEN02	F	327	13/01/2014	Valle Morosina (PD)	10/48	211
VEN03[†]	F	355	13/01/2014	Valle Morosina (PD)	6/16	513
VEN04	F	361	13/01/2014	Valle Morosina (PD)	10/48	141
VEN05*	F	339	13/01/2014	Valle Morosina (PD)	10/48 on-off	805
VEN06	F	373	18/01/2015	Valle Morosina (PD)	6/16	257
VEN07[†]	F	375	18/01/2015	Valle Morosina (PD)	6/16	228
VEN09	F	337	18/01/2015	Valle Morosina (PD)	6/16	192
VEN10	F	348	18/01/2015	Valle Morosina (PD)	6/16	283
VEN12	F	389	09/01/2016	Valle Morosina (PD)	10/48 on-off	151
VEN13	F	391	08/01/2016	Valle Morosina (PD)	10/48 on-off	180
VEN14	M	445	08/01/2016	Valle Morosina (PD)	10/48 on-off	368
VEN15	M	446	07/01/2016	Valle Morosina (PD)	10/48 on-off	136
VEN16[†]	M	381	18/01/2016	Valle Morosina (PD)	10/48 on-off	41

VEN17	F	415	18/01/2016	Valle Morosina (PD)	10/48 on-off	280
VEN18	F	403	16/01/2017	Valle Morosina (PD)	10/48 on-off	159
VEN19†	F	386	16/01/2017	Valle Morosina (PD)	10/48 on-off	66

† Individuals that did not complete the migration because they were shot, or the instrument stopped transmitting abruptly.

Table S2. Environmental datasets used in the analyses.

Data	Data provider	Dataset	Spatial resolution	Temporal resolution	Used in analysis
Soil Temperature (first level: 0-7cm)	ECMWF (European Centre for Medium-Range Weather Forecasts global)	ERA5-Land hourly data from 1950 to present	9 km	Hourly	Wintering grounds, stopovers
Relative humidity	ECMWF	ECMWF Global Atmospheric Reanalysis (ERA-Interim)	~ 70 km	Daily	Wintering grounds
Cloud cover percentage	ECMWF	ECMWF Global Atmospheric Reanalysis (ERA-Interim)	~ 70 km	Daily	Wintering grounds, Stopovers
Wind components 3 pressure levels	ECMWF	ECMWF Global Atmospheric Reanalysis (ERA-Interim)	~ 70 km	6 h (6 – 12 PM)	Wintering grounds, Stopovers
Precipitation	ECMWF	ECMWF Global Atmospheric Reanalysis (ERA-Interim)	~ 70 km	Daily	Wintering grounds, Stopovers
Atmospheric Pressure	ECMWF	ERA5-Land hourly data from 1950 to present	9 km	Hourly	Wintering grounds Stopover
Freeze/thaw grounds	NSIDC (National Snow and Ice Data Center)	MEaSUREs Global Record of Daily Landscape Freeze/Thaw Status (Version 5)	25 km	Daily	Stopover

Table S3. Model selection for the Cox proportional hazards model on departure from wintering sites of teal tagged in Italy from 2013 to 2018. The model selection was performed keeping fixed the variables: photoperiod (Daylength), residuals of temperature (RSoilTemp) and wind v-component at atmospheric pressure level 1000 mPa (Vwind). These variables were expected to have an effect on teal's departure decision. We also imposed to the model selection a maximum number of fixed variables of four in order to avoid overparametrization. For each model we have reported ΔAICc (difference in AICc between a given model and the model with the lowest AICc) and Akaike weights (w_i). Concordance (± SE), model significance [Wald test], model coefficients (β ± SE) and relative significance, estimated hazard ratio (HR) of departure after 1 SD increase of the variables included in the model (95% coefficient intervals) are reported only for the best model, as the other models deviate by more than two AICc units from the best one. Number of observations = 1876; number of individuals = 30.

Model	**ΔAICc**	**w_i**	**Concordance**	**Wald test**	**Daylenght**	**RSoilTemp**	**Vwind**	**Cloud cover**
Daylength + RSoilTemp + Vwind	0.00	0.38	0.68 ± 0.07	9.95, df = 3, p = 0.02	β = 1.29 ± 0.61, z = 2.58, p = 0.009 HR = 3.63 (1.369.6)	β = 0.17 ± 0.26, z = 0.81, p = 0.41 HR = 1.19 (0.78-1.813)	β = 0.180 ± 0.10, z = 1.72, p = 0.08 HR = 1.20 (0.97-1.48)	-
Daylength + RSoilTemp + Vwind + Cloud cover	1.87	0.15	0.69 ± 0.06	10.18, df = 4, p = 0.04	β = 1.24 ± 0.62, z = 2.41, p = 0.01 HR = 3.46 (1.26-9.48)	β = 0.20 ± 0.26, z = 0.93, p = 0.35 HR = 1.22 (0.79-1.90)	β = 0.17 ± 0.10, z = 1.61, p = 0.10 HR = 1.19 (0.96-1.48)	β = -0.19 ± 0.21, z = -1.08, p = 0.27 HR = 0.82 (0.58-1.16)
Daylength + RSoilTemp + Vwind + Uwind	*2.19*	*0.12*						
Daylength + RSoilTemp + Vwind + Relative humidity	*2.29*	*0.12*						
Daylength + RSoilTemp + Vwind + Precipitation	*2.51*	*0.11*						
Daylength + RSoilTemp + Vwind + Atmospheric pressure	*2.66*	*0.10*						

Table S4. Model selection for the GEE model on departure from stopover sites of teal tagged in Italy from 2013 to 2018. The model selection was performed keeping fixed the variables: Defrost Degree Day (DDD) and wind v-component (Vwind), that were expected to have an effect on teal's departure decision. We also imposed to the model selection a maximum number of fixed variables of three in order to avoid overparametrization. The models are here reported from the lowest value of QIC. Number of observations = 1050; number of individuals = 21.

Model	**deltaQIC**	**weight**
DDD + Vwind + Cloud cover	0.0	0.963
DDD + Vwind + Precipitation	*8.1*	*0.017*
DDD + Vwind	*9.4*	*0.009*
DDD + Vwind + atmospheric pressure	*10.1*	*0.006*
DDD + Vwind + Uwind	*10.4*	*0.005*

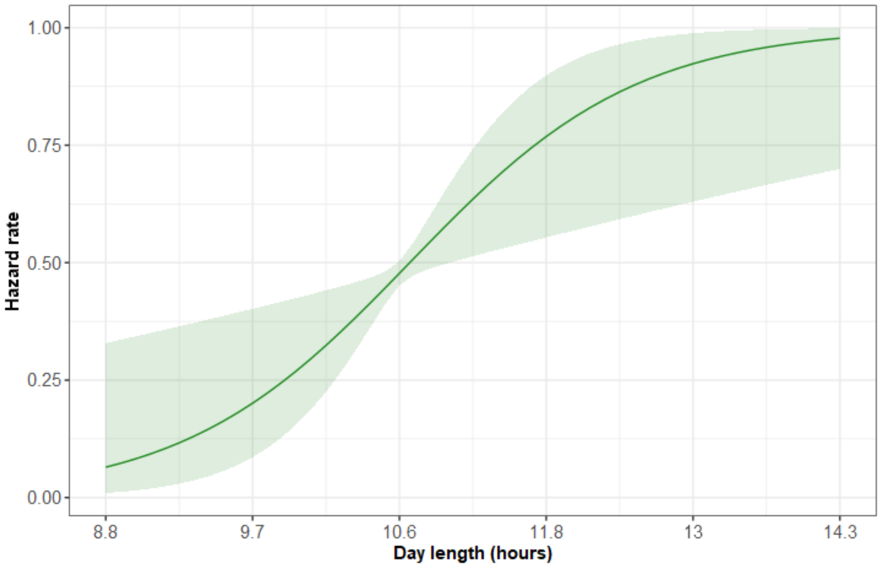

Fig. S1 Plot of the effects of day length (hours) (RSoilTemp = -0.0 °C, wind v-component = -0.49 m/s, cloud cover = -0.0) on the probability of departure from wintering areas. Shaded areas = 95% confidence bands. Results from the best Cox proportional hazard model developed to describe the factors affecting the departure from wintering areas for spring-migrating teal tagged in Italy from 2013 to 2018. Number of birds: 30. See Table S3 for numerical results.

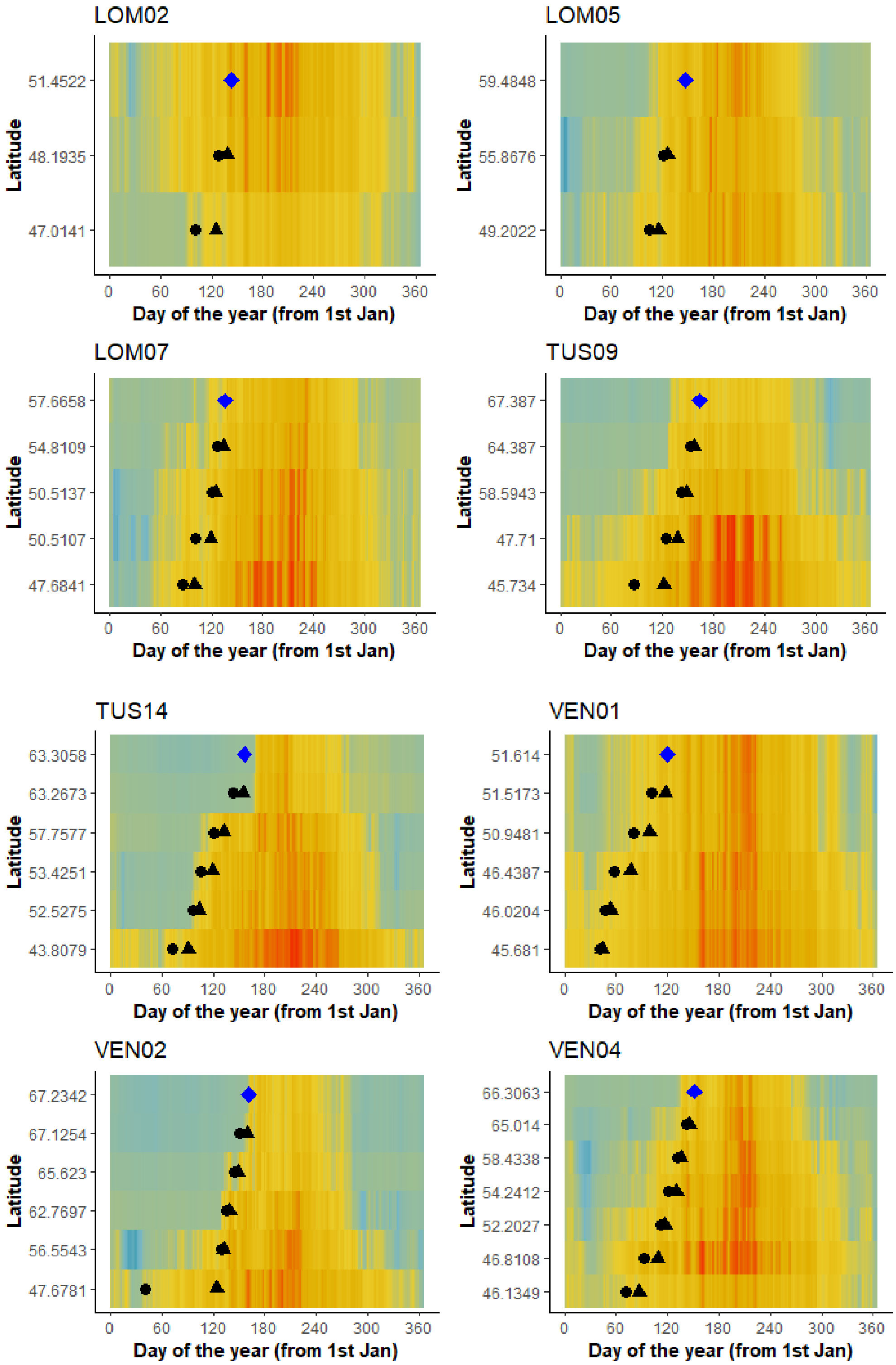
LOM02
51.4522
48.1935
47.0141
Latitude
0
60
120
180
240
300
360
Day of the year (from 1st Jan)
LOM05
59.4848
55.8676
49.2022
Latitude
0
60
120
180
240
300
360
Day of the year (from 1st Jan)
LOM07
57.6658
54.8109
50.5137
50.5107
47.6841
Latitude
0
60
120
180
240
300
360
Day of the year (from 1st Jan)
TUS09
67.387
64.387
58.5943
47.71
45.734
Latitude
0
60
120
180
240
300
360
Day of the year (from 1st Jan)
TUS14
63.3058
63.2673
57.7577
53.4251
52.5275
43.8079
Latitude
0
60
120
180
240
300
360
Day of the year (from 1st Jan)
VEN01
51.614
51.5173
50.9481
46.4387
46.0204
45.681
Latitude
0
60
120
180
240
300
360
Day of the year (from 1st Jan)
VEN02
67.2342
67.1254
65.623
62.7697
56.5543
47.6781
Latitude
0
60
120
180
240
300
360
Day of the year (from 1st Jan)
VEN04
66.3063
65.014
58.4338
54.2412
52.2027
46.8108
46.1349
Latitude
0
60
120
180
240
300
360
Day of the year (from 1st Jan)

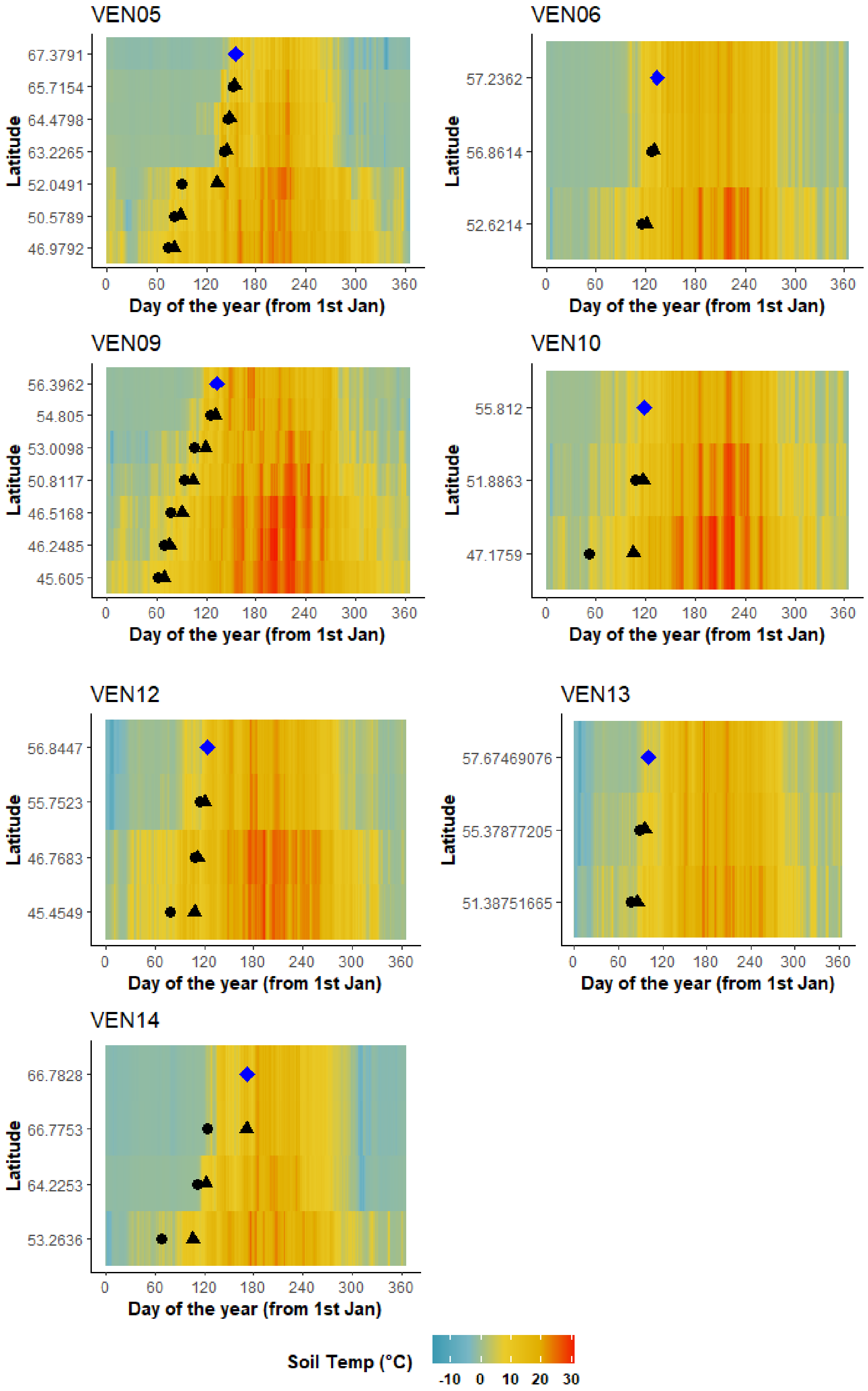

Fig. S2 Spatio-temporal matrixes of soil temperatures for each stopover frequented by teal and breeding site. The x-axis represents "time" as day of the year from the 1 January, while the y-axis represents "space" as the latitude of the stopover frequented by each teal. The last latitude reported is the latitude of the breeding area. The colour gradient represents the soil temperatures recorded in each stopover (latitude) and time of year. The black dots and triangles indicate the day of year when the teal arrived and left the stopover area respectively. The blue diamond shows the arrival day at the breeding site. The data for VEN05 refers only to spring migration for year 2014, that was used in all the analysis.

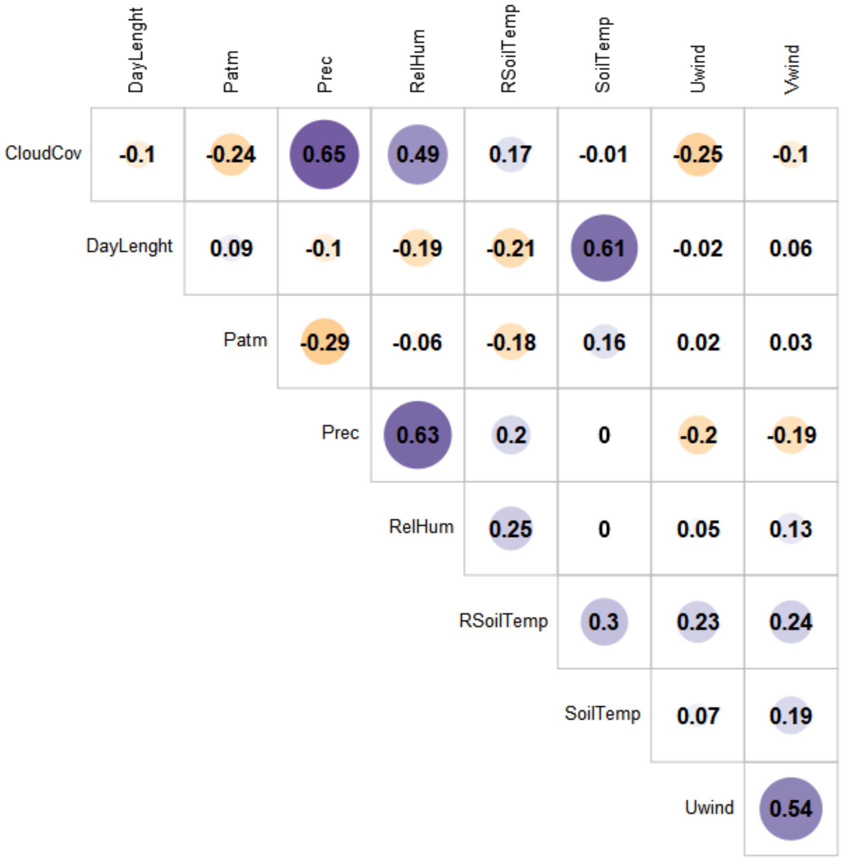

	DayLenght	Patm	Prec	RelHum	RSoilTemp	SoilTemp	Uwind	Vwind
CloudCov	-0.1	-0.24	0.65	0.49	0.17	-0.01	-0.25	-0.1
DayLenght		0.09	-0.1	-0.19	-0.21	0.61	-0.02	0.06
Patm			-0.29	-0.06	-0.18	0.16	0.02	0.03
Prec				0.63	0.2	0	-0.2	-0.19
RelHum					0.25	0	0.05	0.13
RSoilTemp						0.3	0.23	0.24
SoilTemp							0.07	0.19
Uwind								0.54

Fig. S3 Correlation between environmental variables considered as potential cues for the departure from wintering areas of teal tagged in Italy between 2013 and 2018. The correlation between variables reported in the plot was evaluated using Spearman correlation test. Uwind and Vwind represent the u and v wind components respectively, at altitude of 1000 mPa.

Fig. S4 Correlation between environmental variables considered as potential cues for the departure from stopover sites of teal tagged in Italy between 2013 and 2018. The correlation between variables reported in the plot was evaluated using Spearman correlation test. DDD is the Defrost Degree Day, while Uwind and Vwind represent the u and v wind components respectively, at altitude of 1000 mPa.